

# Adaptive Step Duration for Precise Foot Placement: Achieving Robust Bipedal Locomotion on Terrains with Restricted Footholds

Zhaoyang Xiang<sup>1</sup>, Victor Paredes<sup>1</sup>, and Ayonga Hereid<sup>1</sup>

**Abstract**—This paper introduces a novel multi-step preview foot placement planning algorithm designed to enhance the robustness of bipedal robotic walking across challenging terrains with restricted footholds. Traditional one-step preview planning struggles to maintain stability when stepping areas are severely limited, such as with random stepping stones. In this work, we developed a discrete-time Model Predictive Control (MPC) based on the step-to-step discrete evolution of the Divergent Component of Motion (DCM) of bipedal locomotion. This approach adaptively changes the step duration for optimal foot placement under constraints, thereby ensuring the robot’s operational viability over multiple future steps and significantly improving its ability to navigate through environments with tight constraints on possible footholds. The effectiveness of this planning algorithm is demonstrated through simulations that include a variety of complex stepping-stone configurations and external perturbations. These tests underscore the algorithm’s improved performance for navigating foothold-restricted environments, even with the presence of external disturbances.

## I. INTRODUCTION

Humanoid and bipedal robots are developed to collaborate with humans while navigating through human environments built to perform their daily activities. They are expected to achieve robust and efficient locomotion similar to humans as they navigate challenging terrain, such as slopes, stairs, stepping stones, etc. However, the dynamics of bipedal robots are inherently high-dimensional, nonlinear, and hybrid with unilateral contact constraints, which remains a complex problem for planning stable trajectories ahead.

An efficient approach to characterizing bipedal locomotion has been using the reduced-order center of mass (CoM) dynamics models to represent the robot dynamics, which can then generate walking patterns or lower-limb trajectories. The most commonly used model, the linear inverted pendulum model (LIPM), describes the CoM dynamics with a constant CoM height and underactuated ankles in a linear form [1], [2]. Kajita et al. use LIPM with zero momentum point (ZMP) regulations to avoid falling and achieve stable 3D walking on flat ground [3], [4]. Paredes et al. and Xiong et al. analyze the closed-form orbit behaviors of the 3D LIPM model and use it to stabilize the walking gaits of more complex models or real robots [5], [6]. Moreover, the angular momentum-based linear inverted pendulum (ALIP) model reportedly improves the representation of linear velocities of the CoM using the angular momentum of the robot about

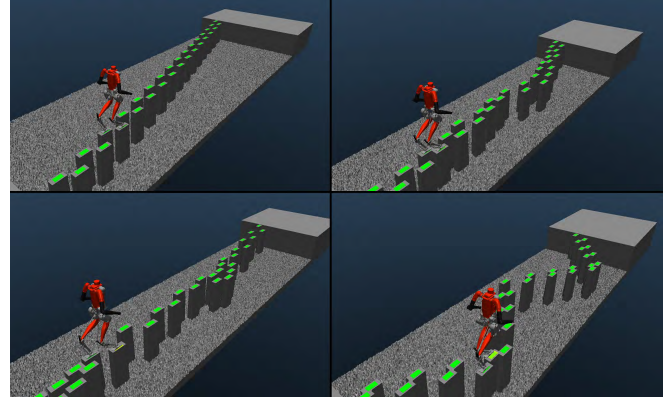


Fig. 1. Digit robot stably walks across a variety of challenging stepping stone configurations in simulation by dynamically adjusting both step duration and stepping locations.

the contact point [7], which reduces the error between the model and real robots and improves the robustness of the foot placement control [8]. Although most of these works assume the ALIP model to be on flat ground, it can be generalized to more complicated terrain. Gibson et al. designed a novel set of constraints of the ALIP model for slope walking and formulated a model predictive control (MPC) problem for foot placement control [9]. Gao et al. extend the ALIP model to consider swaying rigid surfaces and stabilize the robot using a feedback linearization-based controller [10].

More specifically, a random and constrained terrain characterized by stepping stones is a typical problem in bipedal robotic walking. Nguyen et al. pre-computed a gait library using trajectory optimization for fixed stepping stone profiles with various distances and heights and generated the interpolated gaits online for given stepping stones [11]. Li et al. follow a similar path but formulate a whole-body control optimization problem to adapt the gait library to given stepping stones [12]. Dai et al. consider the orbital energy of the ALIP model on slopes and use MPC to generate the CoM trajectory on stepping stones with variable heights [13]. Nonetheless, it remains a complex question about how adaptive the walking control algorithms can be to random stepping stones.

To analyze the stability of LIPM-like CoM dynamics models, the capturability [14] and the Divergent Component of Motion (DCM) [15] are introduced to decouple the stable and unstable dynamics, which provides a criterion based on the viable states (i.e., states that do not lead to falling). As those analyses show, a variable step duration

\*This work was supported in part by the National Science Foundation under grant FRR-21441568.

<sup>1</sup>Mechanical and Aerospace Engineering, Ohio State University, Columbus, OH, USA. (xiang.295, paredescauna.1, hereid.1)@osu.edu.

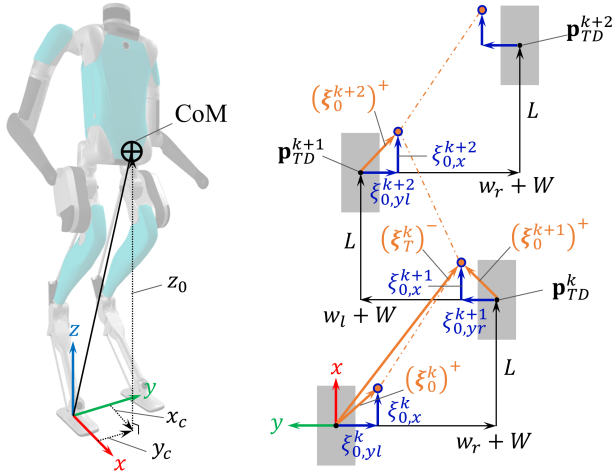


Fig. 2. (Left) Digit robot and the ALIP model; (Right) Schematic view of the DCM with step positions and footprints: During the  $k$ -th step, the DCM evolves from  $(\xi_0^k)^+$  to  $(\xi_T^k)^-$  and is reset to  $(\xi_0^{k+1})^+$  in the new contact frame after the touch-down, and so repeatedly.

can increase the range of viable states and allow robots to take wider steps to prevent falling. However, allowing a variable step duration leads to nonlinear and non-convex problems, which require heavy computing resources and thus impede its implementation in online controllers. The aforementioned research [11], [12], [13] all assume variable step duration to increase the robustness of walking gaits, but they do not explicitly analyze or optimize it due to the same reason. As a novel attempt, Khadiv et al. introduce the DCM offset to represent the viability bounds of the LIPM model and formulate the desired step position, step duration, and DCM offset into online quadratic programming (QP) [16]. This foot placement controller ensures bounded viable states while seeking an optimal stepping strategy, improving the walking control's robustness, especially under force perturbations. This work is also extended for more complicated stepping strategies [17] or more challenging walking perturbation [18], which implies its potential application in walking control on stepping stones.

This paper focuses on foot placement planning (also referred to as high-level control sometimes) on flat stepping stones with force perturbation, representing a common type of challenging terrain in the real world. To improve the robustness of bipedal robotic walking on such terrain, we aim to plan a swing foot placement that guarantees viable states of future steps and prevents the robot from falling, given severe constraints on the step position. Thus, we consider variable step duration and analyze the DCM based on the ALIP model. Moreover, one-step-ahead planning strategies (such as [16], [7]) may not guarantee the viability of the next step, given the uncertainty in the terrain. Therefore, we formulate a discrete MPC problem considering  $N$  steps ahead to increase the robustness of walking gaits in future consecutive steps. To validate our approach, we test our foot placement planner on the humanoid robot model, Digit, in

the MuJoCo simulation environment [19] with different types of stepping stone terrains and under force perturbations.

The main contributions of this paper in foot placement planning are as follows:

- 1) Derive the discrete dynamics of the initial DCM based on the ALIP model and prove its boundedness if the foot placements are chosen from a bounded set.
  - 2) Introduce the  $N$ -step-ahead discrete MPC formulation to increase the robustness of the walking gait given the terrain information. This yields a nonlinear programming (NLP) problem with bilinear constraints and thus has the potential to be implemented in online foot placement planning under our construction.
  - 3) Demonstrate the robustness of the foot placement planner in different challenging scenarios, including random stepping stones and severe force perturbations.
- We also compare this work with [16] to show the improvement of considering more steps ahead.

The rest of the paper is organized as follows: Section II derives the evolution of the DCM through consecutive steps and introduces the discrete dynamics of the initial DCM. We show that the DCM can be bounded by the swing foot placement of a particular position and duration, which leads to balanced walking. Section III formulates a discrete MPC by considering multiple steps ahead to solve for a foot placement that maintains the viable states of the following steps. Section IV briefly mentions the whole-body controller we use in the simulation and explains the computation of the low-level desired outputs due to the variable step duration. Section V demonstrates the improvement of the robustness by our planner in four stepping stone profiles and one perturbation test. Lastly, Section VI concludes the paper and provides some potential topics to improve this work.

## II. DIVERGENT COMPONENT OF MOTION ANALYSIS OF BIPEDAL LOCOMOTION

The complex, high-dimensional dynamics of a bipedal robot present significant computational challenges for gait planning. To address these issues, reduced-dimensional template models are commonly employed, offering a simpler representation that mitigates the computational demands of planning bipedal locomotion.

### A. Center of Mass Dynamics of Bipedal Robots

We consider the ALIP model on a flat ground with an underactuated single-support phase and an instantaneous double-support phase (see Fig. 2, Left) [7]. Using  $x_c, y_c, z_0$  to denote the CoM position in the contact point frame, the ALIP dynamics are given by

$$\begin{aligned} \dot{x}_c &= \frac{L^y}{mz_0}, & \dot{y}_c &= -\frac{L^x}{mz_0}, \\ \dot{L}^x &= -mgy_c, & \dot{L}^y &= mgx_c, \end{aligned} \quad (1)$$

where  $z_0$  is the constant CoM height,  $L^x, L^y$  are the  $x, y$ -component of the angular momentum about the contact point (i.e., contact angular momentum),  $m$  is the mass of the robot, and  $g$  is the gravitational acceleration constant. Note that  $L^x$

is in the opposite direction of  $\dot{y}_c$  in the right-hand coordinate system. Compared to the LIP model described in [2], the ALIP model uses the contact angular momentum  $L^x, L^y$  instead of the linear velocities of the CoM. As discussed in [8]–[10], this change maintains the system dynamics in a linear form while reducing the mismatch between the model and the real robot state. Thus, we choose this model to represent the CoM dynamics of the robot in this paper.

## B. DCM-based Discrete Dynamics

The ALIP dynamics in (1) can be transformed into a system that separates the stable and unstable parts of its dynamics, where the latter is its Divergent Component of Motion [15]. Using the states of the ALIP model, the DCM  $\xi$  in the contact frame is given by

$$\xi = \begin{bmatrix} \xi_x \\ \xi_y \end{bmatrix} = \begin{bmatrix} x_c \\ y_c \end{bmatrix} + \frac{1}{\lambda} \frac{1}{mz_0} \begin{bmatrix} L^y \\ -L^x \end{bmatrix}. \quad (2)$$

Substituting the ALIP dynamics (1) into (2), we can obtain the DCM dynamics and solve it as follows

$$\dot{\xi} = \begin{bmatrix} \dot{\xi}_x \\ \dot{\xi}_y \end{bmatrix} = \lambda \begin{bmatrix} \xi_x \\ \xi_y \end{bmatrix}, \quad (3)$$

$$\xi(t) = \xi_0 e^{\lambda t}, \quad t \in [0, T], \quad (4)$$

where  $T$  is the step duration,  $t$  is the elapsed time (or relative time) from the beginning of the current swing phase,  $\xi_0$  is the initial DCM at  $t = 0$ .

The DCM  $\xi(t)$  is an exponential function of the time  $t$  through a walking step, which represents the unstable motion of a walking gait. However, after a swing foot touch-down, the DCM is reset to an initial value due to the update of the contact frame (see Fig. 2, Right). Suppose that the current step is the  $k$ -th step ( $k \in \mathbb{N}$ ),  $(\xi_0^k)^+$  and  $(\xi_T^k)^-$  are the initial and final value of the DCM of the  $k$ -th step, and  $(\xi_0^{k+1})^+$  is the initial value of the  $(k+1)$ -th step<sup>1</sup>, where the superscript  $(+/-)$  represents the moment right after or before the  $k$ -th touch-down. Then, the reset map of the DCM is given by

$$\begin{aligned} (\xi_0^{k+1})^+ &= (\xi_T^k)^- - \mathbf{p}_{TD}^k \\ &= (\xi_0^k)^+ e^{\lambda T^k} - \mathbf{p}_{TD}^k, \end{aligned} \quad (5)$$

where  $\mathbf{p}_{TD}^k = [x_{TD}^k, y_{TD}^k]^T$  is the  $k$ -th step position in the current contact frame,  $T^k$  is the  $k$ -th step duration.

In the  $x$ -direction, the step length  $x_{TD}$  can be positive, zero, or negative when walking forward, in place, or backward respectively. While in the  $y$ -direction, even if the robot is stepping in place, there will be an alternating step width  $w_{l/r}$  in the left or right direction<sup>2</sup>. Thus, we define the lateral step position  $y_{TD} := w_{l/r} + W$ , where  $w_{l/r}$  is a fixed step width of the left or right swing foot that stands for the in-place lateral walking, and  $W$  is the deviation from  $w_{l/r}$  that accounts for the actual lateral movement. For instance, Fig.

<sup>1</sup> $(\xi_0^{k+1})^+$  is also referred to as the DCM offset at the end of the  $k$ -th step in [16].

<sup>2</sup>i.e.,  $w_l = w > 0$  for the left swing foot and  $w_r = -w < 0$  for the right swing foot, and  $w > 0$  is a fixed step width when stepping in place.

2 (Right) shows a rightward walking in the  $y$ -direction with  $W < 0$  for each step.

For a periodic gait with a constant step position  $\mathbf{p}_{TD} = [L, w_{l/r} + W]^T$  and duration  $T$ , the nominal value of the initial DCM  $\xi_{0,\text{nom}}$  can be derived from (5) as

$$\xi_{0,x,\text{nom}} = \frac{L}{e^{\lambda T} - 1}, \quad (6)$$

$$\xi_{0,y_{l/r},\text{nom}} = \frac{w_{l/r}}{e^{\lambda T} + 1} + \frac{W}{e^{\lambda T} - 1}, \quad (7)$$

where  $\xi_{0,y_{l/r},\text{nom}}$  of the left or right swing foot are solved by considering two consecutive steps (i.e., one cycle of lateral walking).

We consider the forward walking in the  $x$ -direction as an example. Given a bounded set  $\mathcal{D}$  of the feasible step position and  $\mathcal{T}$  of the feasible step duration, we can obtain a bounded set  $\mathcal{X}$  of the initial DCM computed by the values in  $\mathcal{D}$  and  $\mathcal{T}$  using (6), i.e.,  $\xi_{0,x}(L, T) : \mathcal{D} \times \mathcal{T} \rightarrow \mathcal{X}$ , for all  $L \in \mathcal{D}$ ,  $T \in \mathcal{T}$ . We claim that *the initial DCM  $\xi_{0,x}^k$  evolving from  $\mathcal{X}$  using (5) can be bounded in  $\mathcal{X}$  if the robot takes an appropriate step of a particular position and duration within the set  $\mathcal{D} \times \mathcal{T}$* . To show this, we assume the maximum of the initial DCM to be  $\xi_{0,x,\text{max}}$  that is obtained by the maximal step length  $L_{\text{max}}$  and the minimal step duration  $T_{\text{min}}$ . Then, for  $\xi_{0,x}^k \leq \xi_{0,x,\text{max}}$ , the bound of  $\xi_{0,x}^{k+1}$  is given by (5) as

$$\begin{aligned} \xi_{0,x}^{k+1} &= \xi_{0,x}^k e^{\lambda T^k} - p_{x,TD}^k \\ &\leq \xi_{0,x,\text{max}} e^{\lambda T^k} - p_{x,TD}^k \\ &= \frac{L_{\text{max}}}{e^{\lambda T_{\text{min}}} - 1} e^{\lambda T^k} - p_{x,TD}^k \end{aligned} \quad (8)$$

for any  $p_{x,TD}^k \in \mathcal{D}$  and  $T^k \in \mathcal{T}$ . If the robot takes the next step of the maximal step length  $L_{\text{max}}$  and the minimal step duration  $T_{\text{min}}$ , then the bound of  $\xi_{0,x}^{k+1}$  is limited to

$$\begin{aligned} \xi_{0,x}^{k+1} &\leq \frac{L_{\text{max}}}{e^{\lambda T_{\text{min}}} - 1} e^{\lambda T_{\text{min}}} - L_{\text{max}} \\ &= \xi_{0,x,\text{max}} \end{aligned} \quad (9)$$

thus proves our proposition above.

The infimum of  $\xi_{0,x,\text{max}}$  is also referred to as the  $\infty$ -step capturability bound  $d_\infty$  in [14] (or viability bound) that theoretically distinguishes the stable walking gaits from the unstable ones, and such a bounded evolution of the DCM represents a walking gait that never falls. Furthermore, it can be proved that there exists at least one combination of the step position and duration in  $\mathcal{D} \times \mathcal{T}$  such that the initial DCM  $\xi_{0,x}^k$  in the interior of  $\mathcal{X}$  is a contraction map for  $k \in \mathbb{N}^+$ , which implies a convergent evolution of the initial DCM. The same result also holds for backward walking.

Similarly, we can also compute the boundary values  $\xi_{0,y_{l/r},\text{max}}$  in the  $y$ -direction of the left or right swing foot respectively, and show a bounded evolution of  $\xi_{0,y}^k$  in one cycle of the lateral walking. The details of the proof are omitted in this paper.

Now we define  $\mathbf{z}^k := \xi_0^{k+1}$  (i.e., the initial DCM of the  $(k+1)$ -th step),  $\mathbf{u}^k := \mathbf{p}_{TD}^k$ , and  $\sigma^k := e^{\lambda T^k}$ , and re-write

(5) as the discrete dynamics of the initial DCM through consecutive walking steps:

$$\mathbf{z}^k = \sigma^k \mathbf{z}^{k-1} - \mathbf{u}^k, \quad k = 1, 2, \dots \quad (10)$$

where  $\mathbf{z}^0 = \boldsymbol{\xi}_0^1 = \boldsymbol{\xi}(0)$  is the initial DCM of the current step. In other words, during the stable walking, the initial DCM of the next step  $\mathbf{z}^k$  is determined by the initial value of the current step  $\mathbf{z}^{k-1}$ , the step duration represented by  $\sigma^k$ , and the step position  $\mathbf{u}^k$ .

As we discussed above, for a walking gait starting with an appropriate  $\mathbf{z}^0$ , we can choose the combinations of step position and duration according to (10) to keep all the  $\mathbf{z}^k$  and thus the DCM  $\boldsymbol{\xi}(t)$  bounded such that the robot can walk stably without falling. Even though there are specific constraints on  $\mathcal{D}^k$  and  $\mathcal{T}^k$  for the  $k$ -th step, there still exists at least one swing foot placement that leads to a bounded  $\mathbf{z}^k \in \mathcal{X}^k$  as long as  $\mathbf{z}^{k-1} \in \mathcal{X}^k$ , where  $\mathcal{X}^k$  is obtained by  $\mathcal{D}^k$  and  $\mathcal{T}^k$  using (6). This intuitively indicates a foot placement planning strategy on some challenging terrain such as stepping stones.

### C. Multi-step Ahead Foot Placement Planning

The foot placement planning aims to achieve robust bipedal walking on random stepping stone profiles, which can be modeled as a sequence of bounds on each step position. In that case, the stepping stone profile brings much more complicated constraints on the viable evolution of the robot states, where the robot cannot take steps freely just to maintain balance for the next step. It needs to plan a foot placement in a bounded region based on the states given by the previous bounded foot placement and maintain its viable states to prepare for future bounded foot placements. One-step-ahead planning algorithms can not meet this requirement since they are unaware of the constraints of the far future steps.

The discrete dynamics of the initial DCM (10) reveals that the robot can achieve stable walking on a given stepping stone profile by choosing the appropriate step position and duration to bound the evolution of the initial DCM, which can be implemented as an MPC of the decision variables  $(\mathbf{z}^k, \sigma^k, \mathbf{u}^k)$  that considers multiple steps ahead to solve for the optimal foot placement while minimizing the errors from the desired values. In Section III, we compute the desired and boundary values of the decision variables using the control targets, the terrain information, and the robot states and then formulate the foot placement planner as a discrete MPC. In Section IV, we use an existing whole-body controller to regulate the robot's CoM dynamics and swing foot trajectories to achieve the desired foot placements, forming a closed-loop walking control framework.

## III. SWING FOOT PLACEMENT PLANNING VIA DISCRETE MODEL PREDICTIVE CONTROL

In this work, we focus on the foot placements on the stepping stones with high accuracy and resistance to external perturbations. We consider  $N$  steps ahead to formulate the MPC based on (10), and design the constraints on the decision variables as follows.

1) **Step Position:** For the Digit robot model with under-actuated ankles and flat feet, we define the step position  $\mathbf{u}^k$  as the geometric center of each stance foot. A stepping stone profile is given as a sequence of fixed positions in the world frame, while the robot states and variables such as the DCM and the step position are defined in each contact frame. Considering the next  $N$  stepping stones, the target is to minimize the error between the future step position  $\mathbf{u}^k$  and stepping stone  $\mathbf{p}_{stone}^k$  for  $k = \{1, 2, \dots, N\}$ . Thus, the desired values of each step position are computed as

$$\mathbf{u}_{des}^k = \begin{cases} \mathbf{p}_{stone}^1 - \mathbf{p}_{ST,wld}, & k = 1 \\ \mathbf{p}_{stone}^k - \mathbf{p}_{TD,wld}^{k-1}, & k = 2, \dots, N \end{cases} \quad (11)$$

where  $\mathbf{p}_{ST,wld}$  is the current contact position in the world frame,  $\mathbf{p}_{TD,wld}^{k-1}$  is the expected step position of the future  $(k-1)$ -th step in the world frame. Since the future touch-downs have not happened yet,  $\mathbf{p}_{TD,act}^{k-1}$  are unknown during the current step. However, we can use the previous planning results to approximate these actual values, which are iteratively updated inside the planner. In practice, if the planner has not returned the first result yet, we use the position of the  $k$ -th stone in the  $(k-1)$ -th stone frame to represent each desired step position  $\mathbf{u}_{des}^k$ .

Moreover, the bound on each step position is defined as a rectangular area around the  $\mathbf{u}_{des}^k$ , which represents the physical dimension of the stepping stone.

2) **Step Duration:** Since we emphasize the accuracy of the step position and viability of the walking gait, we make the step duration a slack variable to relax the problem. We choose a constant desired value  $T_{des}^k = T_{des}$  and a constant bound  $[T_{min}, T_{max}]$  for  $T^k$ , and assign a small weight for the step duration term  $\sigma^k$  in the cost function.

3) **Initial DCM:** The desired value of the initial DCM  $\mathbf{z}^k$  are computed using (6) by substituting the desired values of the step position and duration of  $k$ -th step. The bounds of the initial DCM are obtained using the mechanical limits of the robot model, which rules out all the infeasible states that lead to the robot falling (see Appendix for the computation of the  $\mathbf{z}^k$  bounds). However, these bounds alone do not guarantee foot placements that yield viable states for all the given stepping stones. Therefore, we choose an appropriately high weight in the cost term for each  $\mathbf{z}^k$  to track the desired value. This works as a soft constraint to enforce a viable evolution of the initial DCM through multiple steps.

Moreover, since this foot placement planner runs multiple times during a step, we use the measured value of the instantaneous DCM  $\boldsymbol{\xi}_{mea}(t)$  to estimate the initial DCM of the current step  $\mathbf{z}^0$  by computing it backward using (4):

$$\mathbf{z}^0 = \boldsymbol{\xi}_0^1 = \boldsymbol{\xi}_{mea}(t)e^{-\lambda t} \quad (12)$$

where  $t \in [0, T^1]$  is the current relative time. Therefore,  $\mathbf{z}^0$  is updated by the robot states in real-time.

4) **Discrete MPC Formulation:** Using (10), (11), (12), and the other constraints defined above, we can formulate

the discrete MPC problem as follows:

$$\arg \min_{\mathbf{z}^k, \sigma^k, \mathbf{u}^k} \sum_{k=1}^N \beta^k \left( \alpha_1^k \|\mathbf{z}^k - \mathbf{z}_{\text{des}}^k\|^2 + \alpha_2^k |\sigma^k - \sigma_{\text{des}}^k|^2 + \alpha_3^k \|\mathbf{u}^k - \mathbf{u}_{\text{des}}^k\|^2 \right) \quad (13)$$

$$\text{s. t. } \mathbf{z}^k = \sigma^k \mathbf{z}^{k-1} - \mathbf{u}^k \quad (14)$$

$$\begin{bmatrix} u_{x,\min}^k \\ u_{yl/r,\min}^k \end{bmatrix} \leq \mathbf{u}^k \leq \begin{bmatrix} u_{x,\max}^k \\ u_{yl/r,\max}^k \end{bmatrix} \quad (15)$$

$$e^{\lambda T_{\min}} \leq \sigma^k \leq e^{\lambda T_{\max}} \quad (16)$$

$$\begin{bmatrix} z_{x,\min} \\ z_{yl/r,\min} \end{bmatrix} \leq \mathbf{z}^k \leq \begin{bmatrix} z_{x,\max} \\ z_{yl/r,\max} \end{bmatrix} \quad (17)$$

where  $k = \{1, 2, \dots, N\}$ , and we used the weights  $\alpha_{1,2,3}^k$  and  $\beta^k$  to represent soft constraints on the decision variable:  $\alpha_{1,2,3}^k$  assigns relative weights on  $(\mathbf{z}^k, \sigma^k, \mathbf{u}^k)$  for the  $k$ -th future step as we discussed above; while  $\beta^k$  is a decaying weight on each future step, addressing the importance of earlier future steps, especially the imminent next one.

Since the discrete dynamics of DCM (10) takes a bilinear form about the decision variables  $(\mathbf{z}^k, \sigma^k, \mathbf{u}^k)$ , we arrive at an NLP problem. It takes a considerably longer time to solve than QP, but thanks to this discrete formulation, it is still possible to be implemented in online foot placement planning. We will explain further in the conclusion that such bilinear constraints can also be relaxed into linear constraints and thus yield a QP program.

In addition, this planner formulation is not limited to a specific type of terrain, it can be implemented in a variety of flat-ground walking control by designing appropriate constraints and weights to represent different control objectives.

#### IV. ADAPTATION OF VARIABLE STEP DURATION IN THE LOW-LEVEL CONTROLLER

The foot placement planner yields the desired step position  $\mathbf{u}^1$  and duration  $T^1$  of the next step at a low frequency during the current swing phase, while the low-level controller is aimed at approaching that step position with the step duration at a high frequency (e.g., 25 Hz and 1000 Hz respectively). In this work, we use a model-based whole-body controller to track the task space outputs and maintain a stable walking gait<sup>3</sup>. The outputs of the low-level controller are defined using the full-order states  $q$  as

$$\mathcal{Y}^a(q) := \begin{pmatrix} \text{torso pitch} \\ \text{base height } z \\ \text{swing foot } x \\ \text{swing foot } y \\ \text{swing foot } z \\ \text{swing foot pitch} \end{pmatrix} \quad (18)$$

where the desired position of the swing foot is generated as a polynomial trajectory ending at the desired step position with the desired step duration.

<sup>3</sup>For more details about this low-level controller, see [20], [21].

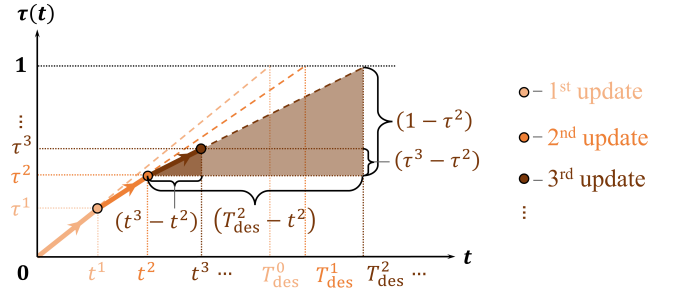


Fig. 3. Illustration of updating  $\tau(t)$  with respect to  $T_{\text{des}}^i$ . For instance, when  $T_{\text{des}}^2$  is updated,  $\tau(t)$  becomes the linear function that starts from  $\tau^2$  and reaches 1 when  $t = T_{\text{des}}^2$ , but it will end at  $\tau^3$  when  $t = t^3$  and be updated again. Eventually,  $\tau(t)$  will be a piecewise linear function of the relative time  $t$ .

Note that the low-level controller uses a dimensionless phase variable  $\tau$  to drive the trajectories of the robot, which increases monotonically from 0 to 1 during the current swing phase. If the step duration is fixed,  $\tau(t)$  is a linear function of the relative time  $t$  with a fixed slope. When we would like to approach a swing foot placement with a variable step duration that is being updated during the swing phase, we need to compute the phase variable  $\tau$  accordingly.

Let  $m$  be the number of times the planner updates the desired foot placement during a swing phase,  $t^i$  and  $\tau^i$  ( $i = 0, 1, \dots, m$ ) be the relative time and the phase variable at the  $i$ -th planner update. From  $t^0 = 0$  and  $\tau^0 = 0$ , the function  $\tau(t)$  is given by:

$$\tau(t) = \tau^i + (1 - \tau^i) \frac{t - t^i}{T_{\text{des}}^i - t^i}, \quad t \in [t^i, t^{i+1}] \quad (19)$$

where  $T_{\text{des}}^i$  is the  $i$ -th updated desired step duration. Each time the planner updates the step duration,  $\tau(t)$  becomes a linear function with an updated slope as if it would start from  $\tau^i$  and reach 1 when  $t$  reaches  $T_{\text{des}}^i$ . However,  $\tau(t)$  will end at  $\tau^{i+1}$  due to the next planner update at  $t = t^{i+1}$ , and thus  $\tau^{i+1}$  is obtained by substituting  $t = t^{i+1}$  into (19), which is the initial value of the next piece of  $\tau(t)$  (See Fig. 3). This design of  $\tau(t)$  guarantees that  $\tau(t)$  is still continuous during each swing phase, and it would eventually reach 1 when  $t$  reaches the last updated step duration, which results in a timely swing foot touch-down. Moreover, the time derivative of the phase variable,  $\dot{\tau}(t)$ , is used to compute the time derivatives of the desired outputs  $\dot{\mathcal{Y}}^{\text{des}}$ ,

$$\dot{\tau}(t) = \frac{1 - \tau^i}{T_{\text{des}}^i - t^i}, \quad t \in [t^i, t^{i+1}]. \quad (20)$$

#### V. SIMULATION RESULTS

This foot placement planner is tested on the humanoid robot model, Digit, in the MuJoCo simulation environment. The simulation runs at 1 kHz, where the low-level controller runs at the same frequency, and the foot placement planner runs every 40 millisecond (i.e., 40 simulation steps). The NLP in the foot placement planner is solved using the open-source NLP solver IPOPT [22]. As a balance between

the planner performance and computational efficiency, we choose the number of future steps considered in the MPC as  $N = 4$ , which includes two cycles of bipedal walking. For all presented simulations, the step position bound is defined as a rectangular area of dimension  $0.2 \times 0.1$  meters centered at each  $\mathbf{u}_{des}^k$ . The step duration takes the desired value of 0.5 seconds with a bound  $[0.35, 0.65]$  seconds. The cost weight for the  $k$ -th step is chosen as  $\alpha^k = [1e4, 2e4, 1, 1e4, 2e4]$  and  $\beta^k = 10^{4-k}$  for  $k = \{1, 2, 3, 4\}$ , where we double the weight in the  $y$ -direction because the step position bound in  $y$ -direction is half of that in  $x$ -direction.

We design 4 types of stepping stone profiles and a perturbation scenario with 4 different perturbations to represent the challenging terrain on the flat ground, where we compare our  $N$ -step-ahead planner (denoted as **ALIP-MPC**) with the one-step-ahead planner (denoted as **ALIP-QP**) in [16]<sup>4</sup>.

TABLE I  
STEPPING STONES PROFILES

Profile No.	$L$ (m)	$W$ (m)
I	constant (0.2/0.4/0.55)	constant $(-0.15/0.15)$
II	$U[0.2, 0.5]$	$U[-0.15, 0.15]$
III	$(0.2*8, 0.5*8)*2$	$U[-0.15, 0.15]$
IV	$U[0.2, 0.5]$	$(-0.1*8, 0.1*8)*2$

#### A. Walking on Stepping Stones

The stepping stone profiles are listed in Table I. Each profile contains 32 stones with the dimensions  $[L^k, W^k]$  to compute the stone position as  $\mathbf{p}_{stone}^k = [L^k, w_{l/r} + W^k]^T$ , where  $w_{l/r}$  is chosen as  $\pm 0.28$  (meters).

- *Profile I* contains 6 combinations of fixed  $L$  and  $W$ ;
- *Profile II* includes  $L$  values that are uniformly distributed random numbers between 0.2 and 0.5, and  $W$  values those between  $-0.15$  and  $0.15$ ;
- *Profile III* contains 8 consecutive  $L$  values of 0.2 followed by 8 values of 0.5 and repeated once, which emphasizes on abrupt changes of stone positions in the  $x$ -direction;
- *Profile IV* emphasize on the stone position changes in the  $y$ -direction similar to *Profile III*.

In the simulation, the robot is initialized in a standing posture with zero velocity and then walks 6 steps to approach the first stepping stone. In this speeding-up phase, we only control the robot to reach an appropriate  $x$ -velocity before walking onto the stepping stones, thus the  $y$ -velocity is near zero and the step position right before the first stone is not constrained. This setting provides an uncertain initial condition for the planner and hence can demonstrate the robustness of the foot placement planning. In each comparison test between the ALIP-MPC and ALIP-QP, we make sure that such initial conditions of either are the same. Therefore, as we will discuss below, the ALIP-MPC outperforms ALIP-QP in all the presented simulation results.

<sup>4</sup>For the video of the presented simulations, see <https://youtu.be/2jhikPlZmBE>.

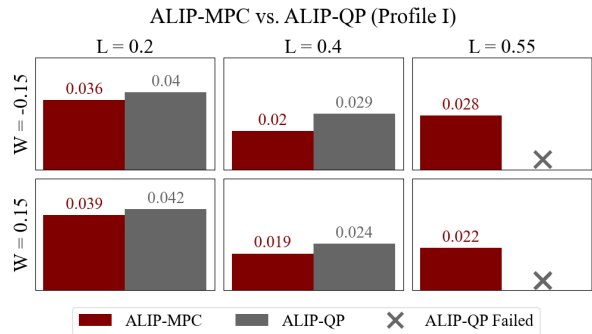


Fig. 4. Step position RMSE of the ALIP-MPC and ALIP-QP in the test of Profile I. The ALIP-MPC outperforms the ALIP-QP in these tests, where the ALIP-QP fails in the tests of large step lengths  $L = 0.55$ .

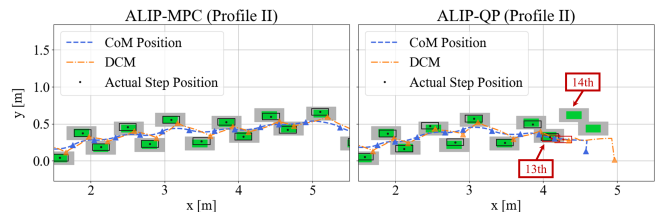


Fig. 5. Footprints of the ALIP-MPC and ALIP-QP in the test of Profile II. The green rectangles mark the step position bounds on the gray stepping stones, the black dots are the actual step positions with the black frames illustrating the flat feet of the Digit. (Left, ALIP-MPC) The robot walks stably through the random stones with a bounded DCM; (Right, ALIP-QP) The robot falls because of a large change in the stone position. The red frames illustrate the foot placements that violate the step position constraints.

1) *Profile I*: The root-mean-square errors between the step positions and stepping stones (abbreviated as step position error below) are illustrated in Fig. 4. For the test of  $L = 0.2$  and  $0.4$ , the ALIP-MPC slightly reduces the step position errors compared to the ALIP-QP. This is because these tests all lead to periodic gaits and thus the preview of multiple steps provides similar information as the one-step preview. However, in the test of  $L = 0.55$ , the step length is very large and close to the mechanical limit. The ALIP-QP fails to obtain a feasible foot placement from an earlier step, which instantaneously results in the infeasibility of the upcoming steps, while the ALIP-MPC can still complete these tests with small step position errors thanks to the preview of multiple steps.

2) *Profile II*: It consists of randomly generated  $L^k$  and  $W^k$ , which is much more challenging for the ALIP-QP to handle. The ALIP-MPC controls the robot to walk through this profile with a step position error of 0.023 meters, while the ALIP-QP ends with the robot falling due to the randomness of the stone positions. Fig. 5 compares the footprints, the CoM, and the DCM trajectories of the ALIP-MPC and ALIP-QP. The ALIP-QP fails at the 14th step because the 13th foot placement yields an initial condition that cannot lead to viable states given the 14th stone position, which again highlights the importance of the multiple-step preview. Fig. 6 compares the step duration and initial DCM in  $y$ -direction of two planners, where the ALIP-MPC can

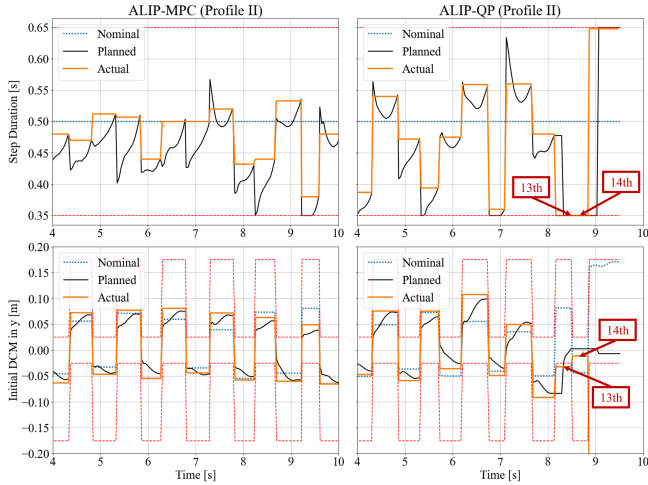


Fig. 6. Step duration and initial DCM of the ALIP-MPC and ALIP-QP in the test of Profile II. (Left, ALIP-MPC) The step duration is adjusted to bound the DCM; (Right, ALIP-QP) The step duration change is large and the ALIP-QP fails to bound the DCM.

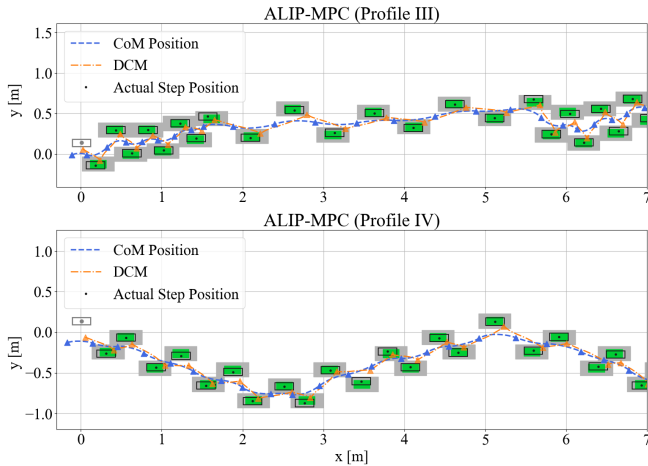


Fig. 7. The ALIP-MPC in the test of Profile III (Upper) and IV (Lower).

find foot placements with more smooth changes in the step duration to maintain viable states.

3) *Profile III and IV*: emphasize on the abrupt changes in the  $L^k$  and  $W^k$  respectively. The step position errors of the ALIP-MPC in these two tests are 0.027 and 0.024 meters, while the ALIP-QP also fails to complete the tests. Fig. 7 shows the footprints of the ALIP-MPC in both tests. Even under such challenging stepping stone profiles, the ALIP-MPC can still find foot placements to maintain viable states.

In all the stepping stones tests, the ALIP-MPC with the preview of multiple steps shows better foot placement tracking and robustness than ALIP-QP, especially when under large changes of stone positions in the lateral direction.

### B. Perturbation Test on Stepping Stones

The perturbations in the  $x$ - and  $y$ -direction are listed in Table II. The test scenario contains 24 steps on the stepping stones profile  $[L^k, W^k] = [0.4, 0]$  and 4 perturbation

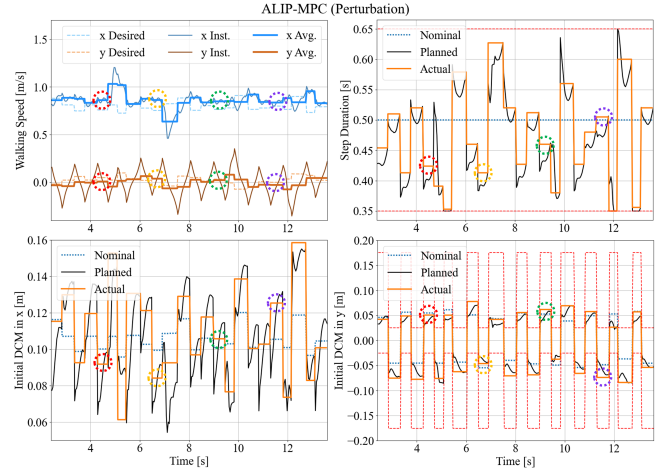


Fig. 8. The ALIP-MPC in the perturbation test, 4 perturbation forces are marked by red, yellow, green, and purple circles respectively in the figures. (Upper Left) The  $x$ - and  $y$ -velocity changes abruptly due to the perturbation but is quickly restored; (Upper Right) The step duration is adjusted in response to the perturbation forces to maintain viable states; (Lower Left and Right) The initial DCM in both  $x$ - and  $y$ -direction are bounded.

TABLE II  
PERTURBATION SCENARIO

Perturb. No.	Step No.	Force (N)
1	5th	$F_x = 150$
2	10th	$F_x = -150$
3	15th	$F_y = 75$
4	20th	$F_y = -75$

forces in the forward, backward, left, and right direction, respectively applied at the base (i.e., the pelvis) of the Digit robot at each specified step. Each perturbation force lasts from the relative time  $t = 0.1$  to  $t = 0.2$  seconds. The results are presented in Fig. 8.

Since we choose a stone profile where the robot walks straightforward, the perturbation resistance of both planners in the  $x$ -direction is similar. When the 1st perturbation force pushes the robot in the forward direction, the robot takes the next step faster than usual. The 2nd perturbation in the backward direction causes the robot to slow down and increases the step duration. Given that the robot has underactuated ankle joints, as long as the perturbation does not completely stop the robot or push the robot forward extremely heavily, both planners can find feasible foot placement to maintain balanced walking. However, for the perturbations in  $y$ -direction, the foot placements are severely constrained by the stepping stones, thus the ALIP-QP fails after the 3rd leftward perturbation. The ALIP-MPC still maintains viable states and completes the test successfully.

## VI. CONCLUSION

This paper presents a discrete MPC formulation for multi-step-ahead foot placement planning that increases the robustness of bipedal robotic walking on challenging terrains. We

choose the ALIP CoM dynamics model to represent the full-order dynamics of the robot more accurately and analyze its viability using the initial DCM of each step. By proving that the initial DCM can be bounded by appropriate foot placements, we introduce an initial DCM discrete dynamics that reveals its evolution under the control of step position and step duration. Then, we formulate the discrete dynamics into an MPC problem for foot placement planning that considers multiple steps ahead, which can use more information about the terrain to plan a foot placement that maintains the viable states through challenging stepping areas. We test our planner on different challenging stepping stone profiles and perturbation scenarios, demonstrating improved robustness than the one-step-ahead planning algorithm. For future works, we will focus on the bilinear constraints in the MPC and use existing relaxation methods to convert it into a QP problem, which will eventually be implemented in the physical robot experiments.

## APPENDIX

We choose the bounds on the mechanical limits of the Digit robot as

$$[T_{\min}, T_{\max}] = [0.35, 0.65](\text{s}), \quad (21)$$

$$[L_{\min}, L_{\max}] = [-0.5, 0.5](\text{m}), \quad (22)$$

$$\begin{aligned} [W_{l,\min}, W_{l,\max}] &= [-W_{r,\max}, W_{r,\min}] \\ &= [-0.18, 0.22](\text{m}). \end{aligned} \quad (23)$$

Then, the  $z_x^k$  bound is computed using (6) as

$$-z_{x,\min} = z_{x,\max} = \frac{L_{\max}}{e^{\lambda T_{\min}} - 1}, \quad (24)$$

The  $z_y^k$  bound of the left or right swing foot is computed by considering two consecutive steps on the boundary as

$$\begin{aligned} z_{yl,\min} &= -z_{yr,\max} \\ &= \frac{w_l}{e^{\lambda T_{\min}} + 1} + \frac{-W_{l,\max} + W_{l,\min} e^{\lambda T_{\min}}}{e^{2\lambda T_{\min}} - 1}, \end{aligned} \quad (25)$$

$$\begin{aligned} z_{yl,\max} &= -z_{yr,\min} \\ &= \frac{w_l}{e^{\lambda T_{\min}} + 1} + \frac{-W_{l,\min} + W_{l,\max} e^{\lambda T_{\min}}}{e^{2\lambda T_{\min}} - 1}. \end{aligned} \quad (26)$$

## REFERENCES

- [1] S. Kajita and K. Tani, "Study of dynamic biped locomotion on rugged terrain-derivation and application of the linear inverted pendulum mode," in *Proceedings. 1991 IEEE International Conference on Robotics and Automation*. IEEE Computer Society, 1991, pp. 1405–1406.
- [2] S. Kajita, F. Kanehiro, K. Kaneko, K. Yokoi, and H. Hirukawa, "The 3d linear inverted pendulum mode: A simple modeling for a biped walking pattern generation," in *Proceedings 2001 IEEE/RSJ International Conference on Intelligent Robots and Systems. Expanding the Societal Role of Robotics in the the Next Millennium (Cat. No. 01CH37180)*, vol. 1. IEEE, 2001, pp. 239–246.
- [3] S. Kajita, F. Kanehiro, K. Kaneko, K. Fujiwara, K. Harada, K. Yokoi, and H. Hirukawa, "Biped walking pattern generation by using preview control of zero-moment point," in *2003 IEEE international conference on robotics and automation (Cat. No. 03CH37422)*, vol. 2. IEEE, 2003, pp. 1620–1626.
- [4] S. Kajita, M. Morisawa, K. Miura, S. Nakaoka, K. Harada, K. Kaneko, F. Kanehiro, and K. Yokoi, "Biped walking stabilization based on linear inverted pendulum tracking," in *2010 IEEE/RSJ International Conference on Intelligent Robots and Systems*. IEEE, 2010, pp. 4489–4496.
- [5] V. C. Paredes and A. Hereid, "Resolved motion control for 3d underactuated bipedal walking using linear inverted pendulum dynamics and neural adaptation," in *2022 IEEE/RSJ International Conference on Intelligent Robots and Systems (IROS)*. IEEE, 2022, pp. 6761–6767.
- [6] X. Xiong and A. D. Ames, "Orbit characterization, stabilization and composition on 3d underactuated bipedal walking via hybrid passive linear inverted pendulum model," in *2019 IEEE/RSJ International Conference on Intelligent Robots and Systems (IROS)*. IEEE, 2019, pp. 4644–4651.
- [7] Y. Gong and J. Grizzle, "One-step ahead prediction of angular momentum about the contact point for control of bipedal locomotion: Validation in a lip-inspired controller," in *2021 IEEE International Conference on Robotics and Automation (ICRA)*. IEEE, 2021, pp. 2832–2838.
- [8] Y. Gong and J. W. Grizzle, "Zero dynamics, pendulum models, and angular momentum in feedback control of bipedal locomotion," *Journal of Dynamic Systems, Measurement, and Control*, vol. 144, no. 12, p. 121006, 2022.
- [9] G. Gibson, O. Dosunmu-Ogunbi, Y. Gong, and J. Grizzle, "Terrain-adaptive, alip-based bipedal locomotion controller via model predictive control and virtual constraints," in *2022 IEEE/RSJ International Conference on Intelligent Robots and Systems (IROS)*. IEEE, 2022, pp. 6724–6731.
- [10] Y. Gao, Y. Gong, V. Paredes, A. Hereid, and Y. Gu, "Time-varying alip model and robust foot-placement control for underactuated bipedal robotic walking on a swaying rigid surface," in *2023 American Control Conference (ACC)*. IEEE, 2023, pp. 3282–3287.
- [11] Q. Nguyen, A. Agrawal, X. Da, W. C. Martin, H. Geyer, J. W. Grizzle, and K. Sreenath, "Dynamic walking on randomly-varying discrete terrain with one-step preview," in *Robotics: Science and Systems*, vol. 2, no. 3, 2017, pp. 384–99.
- [12] J. Li and Q. Nguyen, "Dynamic walking of bipedal robots on uneven stepping stones via adaptive-frequency mpc," *IEEE Control Systems Letters*, vol. 7, pp. 1279–1284, 2023.
- [13] M. Dai, X. Xiong, and A. Ames, "Bipedal walking on constrained footholds: Momentum regulation via vertical com control," in *2022 International Conference on Robotics and Automation (ICRA)*. IEEE, 2022, pp. 10435–10441.
- [14] T. Koolen, T. De Boer, J. Reubla, A. Goswami, and J. Pratt, "Capturability-based analysis and control of legged locomotion, part 1: Theory and application to three simple gait models," *The international journal of robotics research*, vol. 31, no. 9, pp. 1094–1113, 2012.
- [15] J. Engelsberger, C. Ott, and A. Albu-Schäffer, "Three-dimensional bipedal walking control based on divergent component of motion," *Ieee transactions on robotics*, vol. 31, no. 2, pp. 355–368, 2015.
- [16] M. Khadiv, A. Herzog, S. A. A. Moosavian, and L. Righetti, "Walking control based on step timing adaptation," *IEEE Transactions on Robotics*, vol. 36, no. 3, pp. 629–643, 2020.
- [17] R. Zhang, L. Meng, Z. Yu, X. Chen, H. Liu, and Q. Huang, "Stride length and stepping duration adjustments based on center of mass stabilization control," *IEEE/ASME Transactions on Mechatronics*, vol. 27, no. 6, pp. 5005–5015, 2022.
- [18] M.-J. Kim, D. Lim, G. Park, and J. Park, "Foot stepping algorithm of humanoids with double support time adjustment based on capture point control," in *2023 IEEE International Conference on Robotics and Automation (ICRA)*. IEEE, 2023, pp. 12198–12204.
- [19] E. Todorov, T. Erez, and Y. Tassa, "Mujoco: A physics engine for model-based control," in *2012 IEEE/RSJ international conference on intelligent robots and systems*. IEEE, 2012, pp. 5026–5033.
- [20] A. Del Prete, N. Mansard, O. E. Ramos, O. Stasse, and F. Nori, "Implementing torque control with high-ratio gear boxes and without joint-torque sensors," *International Journal of Humanoid Robotics*, vol. 13, no. 01, p. 1550044, 2016.
- [21] G. A. Castillo, B. Weng, S. Yang, W. Zhang, and A. Hereid, "Template model inspired task space learning for robust bipedal locomotion," in *2023 IEEE/RSJ International Conference on Intelligent Robots and Systems (IROS)*. IEEE, 2023, pp. 8582–8589.
- [22] A. Wächter and L. T. Biegler, "On the implementation of an interior-point filter line-search algorithm for large-scale nonlinear programming," *Mathematical programming*, vol. 106, pp. 25–57, 2006.